

1 **Contrasting determinants of mutation rates in germline and soma**

2

3 Chen Chen^{1,2,*}, Hongjian Qi^{3,4}, Yufeng Shen^{3,5}, Joseph Pickrell^{1,2,+}, Molly

4 Przeworski^{1,3,+}

5

6 ¹Department of Biological Sciences, Columbia University, New York, NY

7 ²New York Genome Center, New York, NY

8 ³Departments of Systems Biology, Columbia University Medical Center, New

9 York, NY

10 ⁴Department of Applied Physics and Applied Mathematics, Columbia University,

11 New York, NY

12 ⁵Department of Biomedical Informatics, Columbia University, New York, NY

13 ⁺Co-supervised this project

14 ^{*}To whom correspondence should be addressed: cc3499@columbia.edu

15

16 Keywords:

17 human; mutation rate; germline mutations; somatic mutations; strand asymmetry

18

Abstract

19

20 Recent studies of somatic and germline mutations have led to the identification of
21 a number of factors that influence point mutation rates, including CpG
22 methylation, expression levels, replication timing and GC content. Intriguingly,
23 some of the effects appear to differ between soma and germline: in particular,
24 whereas mutation rates have been reported to decrease with expression levels in
25 tumors, no clear effect has been detected in the germline. Distinct approaches
26 were taken to analyze the data, however, so it is hard to know whether these
27 apparent differences are real. To enable a cleaner comparison, we considered a
28 statistical model in which the mutation rate of a coding region is predicted by GC
29 content, expression levels, replication timing, and two histone repressive marks.
30 We applied this model to both a set of germline mutations identified in exomes
31 and to exonic somatic mutations in four types of tumors. Germline and soma
32 share most determinants of mutations; notably, we detected an effect of
33 expression levels on germline mutations as well as on somatic ones. However,
34 whereas in somatic tissues, increased expression levels are associated with
35 greater strand asymmetry and *decreased* mutation rates, in ovaries and testes,
36 increased expression leads to greater strand asymmetry but *increased* mutation
37 rates. This contrast points to differences in damage or repair rates during
38 transcription in soma and germline.

39

40

Introduction

41

42 Germline mutations are the source of all heritable variation, including in disease
43 susceptibility, and it is increasingly clear that somatic mutations also play

44 important roles in human diseases, notably cancers (Muller 1927; Stratton,

45 Campbell, and Futreal 2009). Understanding the rate and mechanisms by which

46 mutations occur is therefore of interest to both evolutionary biologists and to

47 human geneticists aiming to identify the underlying causes of genetic diseases

48 (Shendure and Akey 2015; Gao et al. 2016). In particular, an accurate estimate

49 of the local mutation rate is key to testing for an excess of disease mutations in

50 specific genes among cases (Lawrence et al. 2013; Samocha et al. 2014).

51 Characterization of the variation in mutation rate along the genome can also yield

52 important insights into DNA damage and repair mechanisms (Stratton 2011;

53 Ségurel, Wyman, and Przeworski 2014).

54

55 Until recently, our understanding of germline point mutations came mainly from

56 analysis of diversity along the genome or divergence among species (Green et al.

57 2003; Webster et al. 2004; Polak and Arndt 2008; Hodgkinson and Eyre-Walker

58 2011; Park, Qian, and Zhang 2012). In the past several years, analyses have

59 also been based on resequencing exomes or whole genomes from blood

60 samples of human pedigrees and identifying variants present in the offspring but

61 absent in the child (reviewed in Campbell and Eichler 2013 and Ségurel, Wyman,

62 and Przeworski 2014; Shendure and Akey 2015; Francioli et al. 2015; Rahbari et

63 al. 2016; Goldmann et al. 2016; Besenbacher et al. 2016). This approach is more
64 direct than analyzing divergence data and presents the advantage of being
65 almost unaffected by selection, but the analysis is technically challenging and,
66 with current study designs, some mutations may be missed, notably those that
67 occur in the early post-zygotic divisions (Rahbari et al. 2016; Moorjani, Gao, and
68 Przeworski 2016; Harland et al. 2016).

69

70 Our knowledge of somatic point mutations, in turn, relies primarily on
71 resequencing tumors. In these analyses, mutation calls are made by sequencing
72 tumor and non-cancerous tissue pairs from the same individual and then
73 excluding the variants shared between the two tissues (as the shared mutations
74 are likely to be germline). Because, in this approach, a large population of cells is
75 sequenced, the mutations identified tend to predate the tumorigenesis and thus
76 are mostly somatic mutations that occurred in normal tissues (see, e.g.,
77 Martincorena et al. 2015; Alexandrov et al. 2015).

78

79 Studies of both germline and soma reveal that the point mutation rate varies
80 across the genome, from the scale of a single base pair to much larger scales
81 (Hodgkinson and Eyre-Walker 2011; Hodgkinson, Chen, and Eyre-Walker 2012;
82 Ségurel, Wyman, and Przeworski 2014). At the single base pair level, the largest
83 source of variation in germline mutation rate is the identity of the adjacent base
84 pairs (Hwang and Green 2004; Hodgkinson and Eyre-Walker 2011). Notably, the
85 mutation rate of CpG transitions (henceforth CpG Ti) is an order of magnitude

86 higher than other mutation types (e.g., Kong et al. 2012). Most CpG dinucleotides
87 are methylated in the human genome; when the methylated cytosine undergoes
88 spontaneous deamination to generate thymine and is not corrected by the time of
89 replication, the damage leads to a mutation. Among other types of sites, rates of
90 mutation vary by 2 to 3 fold (Kong et al. 2012). In the soma, the mutation rate at
91 CpG sites is also elevated, although the extent of the increase differs across
92 tumor types (Pleasance, Stephens, et al. 2010; Pleasance, Cheetham, et al.
93 2010; Lee et al. 2010). More generally, tumors vary in their mutation spectrum:
94 analyses of mutations and their two neighboring base pairs (i.e., considering 96
95 mutation types) point to enrichment of distinct mutational signatures for different
96 types of cancers, a subset of which have been shown to reflect particular
97 mutagens or differences in the efficiency of repair (Alexandrov et al. 2013).
98
99 Over a larger scale of megabases, germline mutation rates have been
100 associated with a number of additional factors, including transcription level (in
101 testis), replication timing (in lymphoblastoid cell lines), chromatin state (both in
102 lymphoblastoid cells and in ovary), meiotic crossover rates and GC content
103 (Hodgkinson and Eyre-Walker 2011; Michaelson et al. 2012; Park, Qian, and
104 Zhang 2012; Francioli et al. 2015; Goldmann et al. 2016; Besenbacher et al.
105 2016). Somatic mutation rates have also been associated with replication timing
106 (in HeLa cell lines) and with average transcription levels across 91 cell lines in
107 Cancer Cell Line Encyclopedia (Lawrence et al. 2013).
108

109 In many cases, little is known about the mechanistic basis for the association of a
110 given factor with mutation rates. However, the association of somatic mutation
111 rates with transcription levels appears to be a byproduct of transcription-coupled
112 repair (TCR), a sub-pathway of nucleotide excision repair (NER) (Hanawalt and
113 Spivak 2008; Nospikel 2009). NER is a versatile repair pathway that senses
114 lesion-causing distortions to DNA structure and excises the lesion for repair.
115 Another subpathway of NER, global genome repair (GGR), can repair lesions on
116 both transcribed strand (henceforth TS) and non-transcribed strand (henceforth
117 NTS), including transcribed regions as well as transcriptionally-silent ones. In
118 contrast, TCR operates only within transcribed regions, triggered by lesions on
119 the TS, which it repairs off the NTS. This mechanism gives rise to a mutational
120 strand asymmetry as well as a compositional asymmetry between strands. For
121 example, TCR leads to more A to G mutations (A>G henceforth) on the NTS than
122 TS; acting over long periods of time, this phenomenon generates an excess of G
123 over A (and T over C) on the NTS (Green et al. 2003; McVicker and Green 2010).
124 Such mutational strand asymmetry has been found in both germline and soma
125 (Green et al. 2003; Polak and Arndt 2008; Rubin and Green 2009; Lawrence et al.
126 2013; Martincorena et al. 2015; Francioli et al. 2015).
127
128 While many of the same determinants appear to play important roles in both
129 germline and soma, there are hints of differences as well. For instance, studies of
130 pre-neoplastic somatic mutations indicate that, over a 100 kb scale, the mutation
131 rates in somatic tissues decrease with expression levels and increase with

132 replication timing (Lawrence et al. 2013). Similarly, two studies that focused on
133 somatic mutations in non-cancerous somatic tissues, normal eyelid tissue and
134 neurons, found mutations to be enriched in regions of low expression and
135 repressed chromatin (Martincorena et al. 2015; Lodato et al. 2015). A similar
136 effect of replication timing was identified in studies of germline mutation
137 (Stamatoyannopoulos et al. 2009; Francioli et al. 2015; Besenbacher et al. 2016;
138 Carlson et al. 2017). However, the effect of expression levels on germline
139 mutation rates remains unclear: one study reported increased divergence
140 between humans and macaques with greater germline expression (Park, Qian,
141 and Zhang 2012), but others found no discernable effect of expression levels on
142 mutation rates (Green et al. 2003; Webster et al. 2004; Polak and Arndt 2008;
143 Hodgkinson and Eyre-Walker 2011; Francioli et al. 2015). This difference
144 between germline and soma is particularly puzzling in light of the observation that
145 the strand asymmetry of mutation rates between TS and NTS is seen in the
146 germline as well as the soma (Pleasance, Cheetham, et al. 2010; Pleasance,
147 Stephens, et al. 2010; McVicker and Green 2010; Lawrence et al. 2013).
148 Together, these observations suggest that the determinants of mutation rates
149 may differ between germline and soma, raising the more general possibility that
150 the damage rate or the repair efficacy differs among cell types (Lynch 2010).
151
152 A limitation, however, is that studies have used different statistical approaches,
153 rendering the comparison hard to interpret. As an illustration, whereas some
154 studies binned the genome into windows of 100 kb (e.g., Lawrence et al. 2013)

155 or 1Mb regions (e.g., Polak et al. 2015), other studies have compared the mean
156 mutation rate in transcribed regions and non-transcribed regions or in genes
157 grouped by expression levels (Hodgkinson and Eyre-Walker 2011; Francioli et al.
158 2015; Lodato et al. 2015). Studies of somatic mutation also vary in whether they
159 group different tissues or distinguish among them (e.g., Pleasance, Stephens, et
160 al. 2010; Lawrence et al. 2013). An additional limitation of earlier studies of
161 germline mutation is that, by necessity, they relied on human-chimpanzee
162 divergence as a proxy for de novo mutation rates (Green et al. 2003; Webster et
163 al. 2004; Hodgkinson and Eyre-Walker 2011), even though divergence reflects
164 not only the mutation process but also effects of natural selection in the human-
165 chimpanzee ancestor and biased gene conversion (McVicker et al. 2009; Duret
166 and Galtier 2009).

167

168 To our knowledge, only one study has used a uniform approach to study
169 germline and soma. Their findings point to possible differences in their
170 determinants: for instance, the histone mark H3K9me3 accounts for more than
171 40% of mutation rate variation at 100 kb in tumors, when a much weaker
172 association is seen in the germline (Schuster-Böckler and Lehner 2012;
173 Goldmann et al. 2016). This analysis relied on pairwise correlations, however,
174 and therefore the results may be confounded by other factors that are correlated
175 to the histone marks and differ between tissues. Moreover, to our knowledge,
176 there has been no parallel treatment of strand asymmetry in germline and soma.

177

178 To overcome these limitations, we built a multivariable regression model, in
179 which the mutation rates of CpG Ti and other types of mutations in a coding
180 region are predicted by GC content, expression levels, replication timing and two
181 histone repressive marks. To this end, we used the expression levels, replication
182 timing and histone marker levels of matched cell types. We applied the model to
183 a large set of germline point mutations identified in exomes from recently
184 published studies on developmental disorders and to somatic point mutations in
185 exomes found in four types of tumors and reported by the Cancer Genome Atlas
186 (see Materials and Methods). In addition, we considered the mutational strand
187 asymmetry in the two sets of data.

188

189

Materials and Methods

190

191 **Datasets.** To study germline mutations, we relied on de novo mutation calls
192 made from 8681 trios surveyed by exome sequencing. We combined results from
193 two main sources: studies of neurodevelopmental disorders (NDD), which
194 considered 5542 cases and 1911 controls (unaffecteds), and studies of
195 congenital heart defect (CHD), conducted by the Pediatric Cardiac Genomics
196 Consortium, which included 1228 trios. The NDD cases include 3953 cases of
197 Autism Spectrum Disorder (ASD), 1133 cases of deciphering developmental
198 disorders (DDD), 264 cases of epileptic encephalopathies (EE), and 192 cases of
199 intellectual disability (ID). All these studies applied similar capture and
200 sequencing methods, and most samples were at >20X coverage (see Table 1).
201 We tested for an effect of the study, which could potentially arise from differences
202 in design or analysis pipeline, by adding a categorical variable (by an analogous
203 approach to the one described below to test for differences among tissues). We
204 found a marginally significant interaction between the study and the expression
205 level in testis (our proxy for expression levels in the germline), driven by one
206 study (CHD cases; Homsy et al. 2015), as well as for interactions between the
207 studies and the effects of H3K9me3 and GC content, driven by two small studies
208 (EE and ID) (see Figure S1). Given these very minor differences and in order to
209 increase our power, we combined all the germline mutation datasets in what
210 follows (see Supplementary Materials Table S1 for list of mutations).

211

Datasets	Trios	References	Capture	Sequencing
Autism Spectrum Disorder (ASD)	3953	De Rubeis et al. 2014; Iossifov et al. 2014	Exome	Illumina and SOLiD
Simons Simplex Collection, unaffected	1911	Iossifov et al. 2014	Exome	Illumina
Congenital heart disease (CHD)	1213	Homsy et al. 2015	Exome	Illumina
Deciphering Developmental Disorders Study (DDD)	1133	The Deciphering Developmental Disorders Study 2015	Exome	Illumina
Epileptic Encephalopathies (EE)	264	Epi4K Consortium and Epilepsy Phenome/Genome Project 2013	Exome	Illumina
Intellectual Disability (ID)	192	de Ligt et al. 2012; Rauch et al. 2012; Hamdan et al. 2014	Exome	Illumina

212 **Table 1.** Summary of germline datasets

213

214 To examine determinants of mutation rates in somatic tissues, we downloaded
215 somatic mutation calls identified in four types of cancer from the Cancer Genome
216 Atlas (TCGA) portal (in July 2015): breast invasive carcinoma (BRCA), cervical
217 squamous cell carcinoma and endocervical adenocarcinoma (CESC), brain lower
218 grade glioma (LGG), and liver hepatocellular carcinoma (LIHC). The numbers of
219 samples are listed below (Table 2). In all cases, both non-cancerous and tumor
220 tissues of patients were sampled and the exomes were sequenced using an
221 Illumina platform. In the studies, mutation calls shared by the normal and tumor
222 samples were removed (on the presumption that they are germline). What
223 remains are somatic mutations found at high enough frequency to be seen in a
224 large population of cells, which are therefore likely to predate the tumorigenesis,
225 i.e., mutations that occurred in the pre-neoplastic tissues (Martincorena et al.
226 2015).

227

228 For each type of cancer with more than one mutation annotation file available in
229 the TCGA data portal, we selected the file that included the largest number of
230 patient samples. We removed the ~7.6% of samples that had an unusually large
231 number of mutations per sample ($p < 0.05$ by Tukey's test), because they are
232 likely to reflect loss of some aspect of the DNA mismatch repair and hence their
233 mutational mechanisms likely differ (Supek and Lehner 2015).

234

Datasets	Sample sizes
Breast Invasive carcinoma (BRCA)	904

Cervical squamous cell carcinoma and endocervical adenocarcinoma (CESC)	181
Low grade glioma (LGG)	502
Liver hepatocellular carcinoma (LIHC)	171

235 **Table 2.** Sizes of TCGA datasets

236

237 **Possible determinants of mutation rates.** We considered the main factors
238 previously reported to be significantly correlated with mutation rates, namely
239 expression levels, replication timing, GC content and histone modification levels.
240 To quantify expression levels, we relied on gene expression data (measured as
241 RPKM) from the Genotype-Tissue Expression (GTEx) for breast, uterus, brain
242 cortex and liver tissues. We used gene expression levels of testis and ovary as
243 our proxy for germline expression.

244

245 The effect of the replication timing on somatic mutation rates was argued to be
246 cell-type specific (Supek and Lehner 2015). We therefore relied on Repli-Seq
247 measurements (provided per base pair) in ENCODE cell lines that match the four
248 types of cancer, namely MCF-7 (breast cancer), Hela-S3 (cervical cancer), SK-N-
249 SH (neuroblastoma), and HepG2 (liver hepatocellular carcinoma) cell lines.

250 These measurements were obtained from the UCSC Genome Browser. In all
251 cases, the replication timing reported is a smooth measure of the relative
252 enrichment of early vs. late S-phase nascent strands, with high values indicating
253 early replication. For each gene, we computed the average replication timing by

254 taking the mean value of the data points that overlap with gene start-to-end
255 coordinates in UCSC Refseq gene database. For genes with multiple transcripts,
256 we took the union of all exons in all transcripts. For germline mutations, there
257 are no data for the appropriate cell types, so we used replicating timing estimates
258 for lymphoblastoid cell lines (LCL) (provided in 10 kb windows) (Koren et al.
259 2012). We also tried using replication timing data from three somatic tissues
260 instead; the replication timing data are highly correlated among the tissues and
261 therefore the effects of mutation were estimated to be very similar (see Figure
262 S2).

263

264 We also considered the effects of chromatin marks that had been shown to
265 correlate individually with somatic and germline mutation rates (Schuster-Böckler
266 and Lehner 2012; Carlson et al. 2017): specifically, histone modification
267 H3K9me3 and H3K27me3, two repressive marks associated with constitutively
268 and facultatively repressed genes, respectively. Levels of these marks were
269 downloaded from roadmap epigenomics data browser (Dec 2015, hg19) and
270 converted to gene-based histone modification levels by averaging across the
271 gene. We used the histone modification levels of adult ovary, breast
272 myoepithelial cells, brain hippocampus and adult liver as proxies for germline,
273 breast, brain and liver, respectively. In the following regression analysis, we
274 considered only three of four somatic tissues, as we could not obtain histone
275 modification data for CESC. Finally, we computed exonic GC content as the
276 fraction of G or C residues in the union of exons in all isoforms of a given gene.

277

278 Germline mutation studies relied on the UCSC Refseq gene annotation, whereas
279 TCGA uses GENECODE annotation, which contains more transcripts (Larsson et
280 al. 2005; Zhao and Zhang 2015). To make the comparison cleaner, we focused
281 on exonic regions considered in both types of studies by using gene and exon
282 coordinates of Refseq database in build hg19 from UCSC genome browser.

283

284 **Statistical model.** Our main goal was to investigate possible relationships
285 between mutation rates and gene expression levels, while controlling for
286 replication timing, GC content and some histone modification levels. Because our
287 mutation counts are over-dispersed, with greater variance than mean, we used a
288 negative binomial regression model (instead of, e.g., a Poisson regression
289 model). Specifically, for every protein-coding gene, we counted the number of
290 CpG Ti or other types of mutations in the coding exons of a gene and treated it
291 as an outcome of a sequence of independent Bernoulli trials with probability λ_i ,
292 where λ_i is the probability of a mutation occurring in gene i .

293

294 Transitions at CpG sites are thought to primarily occur due to spontaneous
295 deamination at methylated cytosines, a distinct mutational source, and thus their
296 determinants may be distinct from other mutation types (reviewed in Ségurel,
297 Wyman, and Przeworski 2014). However, within CpG islands, most CpGs are
298 hypomethylated (Takai and Jones 2002). To focus on a more homogeneous set
299 of methylated CpGs, we therefore excluded CpG islands from the analyses of

300 CpG Ti. CpG island annotations were downloaded from UCSC browser (track:
301 CpG Islands).

302

303 We considered gene expression levels measured in RPKM (X_1), replication
304 timing (X_2), mean histone modification levels (H3K9me3 as X_3 , H3K27me3 as X_4)
305 and GC content (X_5) as predictors. We also included L , the total number of CpG
306 sites (when considering CpG Ti) or all nucleotides (when considering all other
307 types of mutations) in the exons of the given gene, as an exposure variable, to
308 account for the variation in gene length. The logarithm of λ_i is then modeled as a
309 linear combination of these features scores:

$$310 \quad \log(\lambda_i) = \beta_0 + \sum_{j=1}^5 \beta_j X_{ij} + \log(L) + \varepsilon$$

311 We used R function `glm.nb` to estimate the coefficients, where β_0 is an intercept
312 term, β_j is the effect size of feature j , and X_{ij} is the score for feature j in gene i . In
313 order to make the effect sizes of different features comparable within a model,
314 we normalized all the predictor variables to have a mean of 0 and a standard
315 deviation of 1. The gene expression levels measured in RPKM originally range
316 from 0 to a few hundred thousand. As is standard (e.g., Green et al. 2003;
317 Francioli et al. 2015), we added half of the smallest non-zero value in the
318 corresponding expression data sets and then log-transformed the expression
319 level before normalization.

320

321 We note that in this model, we are considering possible effects one at a time.

322 Including interaction terms affects the estimates and significance levels but

323 changes none of the qualitative results, with the exception of results for
324 H3K27me3, which become less significant (see Figure S3).

325

326 To examine whether the predictors have significantly different effects across
327 tissues, we combined the models into one by including a categorical variable C
328 for the tissue type (see Figure 2). In this approach:

329 $C = 1$ for somatic tissues, $C = 0$ for germline;

$$\log(\lambda_{ij}) = \beta_0 + \sum_{j=1}^5 \beta_j X_{ij} + C \left(\beta_6 + \sum_{j=7}^{11} \beta_j X_{ij} \right) + \log(L) + \varepsilon$$

330 X_1, X_2, X_3, X_4 and X_5 are the same genomic or epigenomic features as in the
331 separate model, $\beta_1, \beta_2, \beta_3, \beta_4, \beta_5$ are the effect sizes of features X_1 to X_5 for testis,
332 and $\beta_7, \beta_8, \beta_9, \beta_{10}, \beta_{11}$ are the differences of effect size in the somatic tissue of
333 features X_1 to X_5 compared to those in testis. We used the R function `glm.nb` to
334 estimate the coefficients.

335

336 Similarly, in order to ask whether effects differ between CpG Ti and other type of
337 mutations in the same tissue, we included a binary variable C for the two
338 mutation types (see Figure S4).

339 $C = 1$ for CpG Ti, $C = 0$ for all other mutations;

$$\log(\lambda_{ij}) = \beta_0 + \sum_{j=1}^5 \beta_j X_{ij} + C \left(\beta_6 + \sum_{j=7}^{11} \beta_j X_{ij} \right) + \log(L) + \varepsilon$$

340 All variables are set up the same way as in the combined model described
341 previously, except for that $\beta_7, \beta_8, \beta_9, \beta_{10}, \beta_{11}$ are now the differences of the effect

342 sizes for CpG Ti compared to those for all other mutation types.

343

344 **Mutation spectrum and strand asymmetry analysis.** We annotated the
345 direction of transcription using the UCSC CCDS track and filtered out genes that
346 are transcribed off both strands (1.7% of genes in Refseq), which left around
347 19,000 genes to consider. This annotation allowed us to classify mutations into
348 six types of mutation (A>C, A>G, A>T, G>A, G>C, G>T) on either TS or NTS.
349 There are thus 12 possible changes (each of the six on both strands). We then
350 calculated the mutation rate of any given type on NTS and TS separately, by
351 considering the number of corresponding mutations in the combined data sets,
352 divided by the total number of nucleotides that could give rise to such a mutation
353 in the exons. To obtain the confidence intervals on the mutation rates (reported in
354 Figure 3, 4 and Figure S5) as well as for the mutation asymmetry ratio (Figure 4
355 and Figure S5), we used bootstrap. Specifically, we created 100 samples, of the
356 same size as the original sample, by drawing randomly from the original sample
357 with replacement, and estimated the 95% CI from those 100 samples.
358 We tested for strand asymmetry by a Chi-squared test. Because A>G strand
359 asymmetry shows the greatest asymmetry (Green et al. 2003) and is the only
360 mutation type that we found in all tissues (Figure 3), we focused primarily on this
361 type, though we also considered A>T mutational patterns (see Figure S5). To
362 test if the extent of strand asymmetry changes with transcription levels, we
363 grouped genes into expression level quantiles and calculated A>G strand

364 asymmetry. Our measure of strand asymmetry is the ratio of the mutation rate on
365 NTS to that on TS.

366

367 **Data availability.** Germline mutations are provided in Table S1. TCGA somatic
368 mutations can be downloaded from GDC data portal ([https://gdc-](https://gdc-portal.nci.nih.gov/search/s?facetTab=cases)
369 [portal.nci.nih.gov/search/s?facetTab=cases](https://gdc-portal.nci.nih.gov/search/s?facetTab=cases)). The gene RPKM data are available
370 at GTEx website (<http://www.gtexportal.org/home/datasets>). The replication
371 timing data of LCL and other tissues are available from (Koren et al. 2012) and
372 ENCODE website
373 (https://www.encodeproject.org/search/?type=Experiment&assay_title=Repli-seq)
374 respectively. The histone modification data can be freely accessed at epigenome
375 roadmap website (<http://www.roadmapepigenomics.org/data/tables/all>).

376

377

Results

378

379 We began by applying our multivariable regression model (see Materials and
380 Methods) to compare the determinants of mutation rates per gene between the
381 two germline tissues and among the three somatic tissues (Figure 1). Results for
382 germline mutations are very similar using testis or ovary expression profiles. In
383 both, there is no discernable effect of replication timing, other than a marginally
384 significant negative effect for mutations other than CpG Ti. However, in contrast
385 to a previous study using de novo mutations (Francioli et al. 2013) and most
386 previous studies of divergence, we found a significant increase of germline
387 mutation rates with expression levels for both CpG Ti and other mutation types
388 (Figure 1; see also Figure S2 for similar results with replication timing for different
389 tissues). The difference with a previous analysis of de novo mutations may be
390 due to the scale of a gene considered here (rather than 100 kb windows).

391

392 The effect of expression levels is most clearly seen using testis expression ($P =$
393 0.03 for CpG Ti; $P = 1.4 \times 10^{-5}$ for other mutation types) than using ovary
394 expression, possibly due to the fact that over three quarters of germline
395 mutations are of male origin (Kong et al. 2012; Rahbari et al. 2016; Goldmann et
396 al. 2016). Alternatively, the ovary expression profile may be a poorer proxy for
397 female germ cells than the testis expression profile is for male germ cells. In any
398 case, henceforth, we use testis expression profile for analysis of the germline
399 mutation rates.

400

401 We note that our analysis of germline mutation relies on calls made in exome
402 studies of blood samples from six sets, including five cases and unaffected
403 controls (see Table 1). A previous study reported that in one set of cases,
404 individuals with congenital heart disease (CHD), there is an increased number of
405 putatively damaging mutations in the genes most highly expressed in the
406 developing heart and brain (Homsy et al. 2015). Since the mutations are thought
407 to be germline mutations (rather than somatic mutations), this association cannot
408 be causal, instead reflecting an enrichment of damaging mutations in important
409 heart developmental genes in CHD patients. To evaluate whether our findings of
410 increased mutation rates with germline expression levels could be driven by a
411 similar ascertainment bias, we excluded the CHD set and obtained the same
412 results (see Figure S6). We also reran the analysis, comparing the effects in the
413 five cases compared to the controls; none of the qualitative results differed,
414 though as expected from the smaller size of the control sets, the estimated effect
415 sizes were more uncertain (see Figure S7). Thus, our results suggest that the
416 increase in mutation rates with expression levels in testes is not a result of
417 focusing primarily on cases.

418

419 Germline mutation rates are also associated with H3K27me3 levels. We also
420 found that, other than for CpG Ti, mutation rates in a gene increase with its GC
421 content. This observation is consistent with previous findings of a high rate of GC
422 to AT mutations relative to other types (e.g., Kong et al. 2012). Moreover, it is

423 thought that mis-incorporated bases during DNA replication in an AT rich regions
424 are more easily accessible and thus more easily repaired than GC rich regions
425 (Petruska and Goodman 1985; Bloom et al. 1994). In contrast, we found a
426 marginally negative effect of GC content on germline rates of CpG Ti. A possible
427 explanation for this observation is that spontaneous deamination, the likely
428 source of most CpG Ti, occurs more readily when DNA is single stranded, which
429 is more likely in AT-rich than GC-rich regions (Fryxell and Moon 2005; Elango et
430 al. 2008).

431

432 The effects of determinants on mutation rates are also concordant across
433 somatic tissues. Notably, mutation rates decrease with expression levels in all
434 three tissues, though the magnitudes of the effects differ. This finding is
435 consistent with previous studies and thought to be a result of TCR (Lawrence et
436 al. 2013). Intriguingly, in a model comparing the effects on CpG Ti and other
437 mutation types directly, in all three somatic tissues, the effect of expression levels
438 on mutation rates is most pronounced for CpG Ti (see Figure S4). This finding
439 suggests that damage or repair of CpG Ti is tightly coupled to transcription.

440

441 In all three somatic tissues, there is also a decrease in mutation rate with
442 replication timing and H3K27me3 levels, as well as an increase with H3K9me3
443 levels (Schuster-Böckler and Lehner 2012; Behjati et al. 2014; Blokzijl et al.
444 2016). The effect of replicating timing on mutation rate has been attributed to the
445 depletion of free nucleotides within later replicating regions, leading to the

446 accumulation of single-stranded DNA and thus rendering the DNA more
447 susceptible to endogenous DNA damage (Stamatoyannopoulos et al. 2009). An
448 alternative hypothesis is that DNA mismatch repair (MMR), which is coupled with
449 replication, is more effective in the early replicating regions of the genome; this
450 possibility is supported by the finding that this association is not detected in the
451 tissue of MMR-deficient patients (Supek and Lehner 2015). While on face value,
452 it may seem surprising that replication timing is a significant determinant for the
453 LGG samples, given that neurons are post-mitotic, glial cells still retain their
454 ability to divide and a substantial fraction of mutations detected in neuronal
455 samples may have occurred at earlier stages in development.

456

457 The only difference in the determinants of mutation rates across somatic tissues
458 appears to be the effect of GC content on CpG Ti rates: mutation rates decrease
459 with GC content in brain tissues and increase with GC content in liver and breast
460 tissues. This finding raises the possibility that damage or repair rates of CpG
461 sites differ in brain tissues (Lodato et al. 2015).

462

463 Figure 1 also hints at a difference between testes (also ovaries) and somatic
464 tissues in the directional effect of expression levels on mutation rates, with a
465 marginally significant positive effect for germline mutations ($P = 0.03$ for CpG Ti,
466 $P = 1.4 \times 10^{-5}$ for other mutation types) and a significantly negative effect for
467 somatic tissues (e.g., BRCA: $P = 8 \times 10^{-16}$ for CpG Ti; $P < 2 \times 10^{-16}$ for other mutation
468 types). When we tested for this difference explicitly, by adding a binary variable

469 for soma and germline (see Materials and Methods), we found that expression
470 levels and replication timing differ in their effects, for both CpG Ti and other
471 mutation types (Figure 2).

472

473 Specifically, replication timing has a positive effect on both tissue types but its
474 effect is stronger in soma (Figure 2). The simplest explanation is that a larger
475 fraction of mutations in the soma are introduced by errors related to replication,
476 as opposed to other non-replicative sources. Another (not mutually-exclusive)
477 possibility is that the effect of early replication versus late replication differs to a
478 greater extent in the soma than in the germline. For example, if MMR is much
479 more efficient in early replicating regions (Supek and Lehner 2015) and more
480 efficient in soma than germline.

481

482 To examine this possibility further, we considered a signature of TCR—strand
483 asymmetry—in the different tissues, finding it among germline mutations as well
484 as in all four somatic tissues (Figure 3). Consistent with previous studies (Green
485 et al. 2003; Francioli et al. 2015), one type in particular, A > G, stands out. While
486 the asymmetry is significant in all five data sets, with more mutation on the NTS
487 than the TS, the degree of asymmetry is significantly different among the five
488 data sets (χ^2 test, $P = 3 \times 10^{-8}$), with the strongest seen in germline. Intriguingly,
489 other mutation types, notably G>C mutations, show even more pronounced
490 differences among tissues, with significant excess on the transcribed strand in
491 the germline and LGG samples but a significant paucity on the NTS in BRCA and

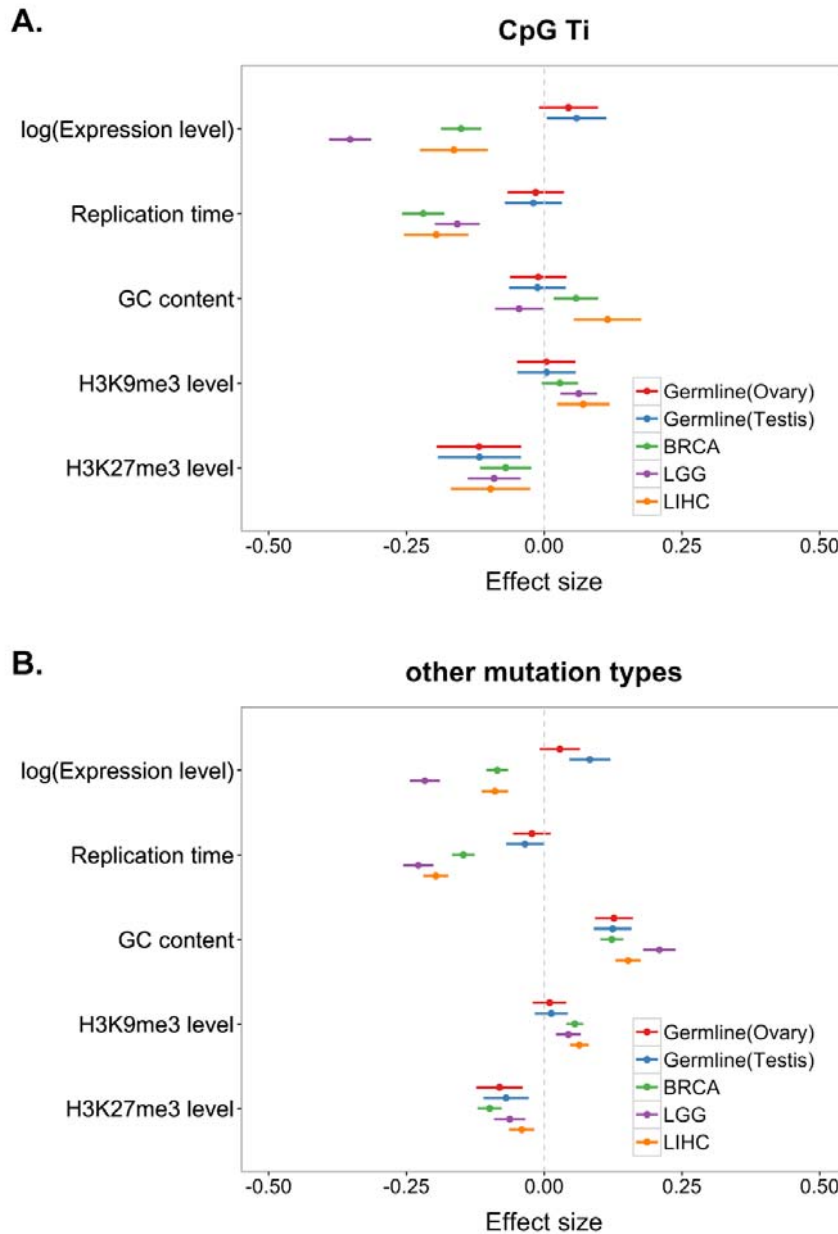
492 CESC. These findings indicate a potential difference in either strand-biased
493 damage or in TCR (or both) among somatic tissues. In summary, the total
494 mutation rate appears to behave quite differently as a function of expression
495 levels in the germline and the soma (Figure 1 and 2), despite the fact that we
496 observed clear evidence for TCR in both types of tissues (Figure 3).

497

498 To examine this difference in more detail, we focused on A>G mutations and
499 considered how the mutation rate and degree of asymmetry covary with
500 expression (Figure 4). A striking contrast emerges: in the germline, as expression
501 levels increase, mutation rates and asymmetry increase, whereas in the soma,
502 asymmetry increases while mutation rates decrease. The same pattern is seen
503 when A>T mutation rate and asymmetry are considered (see Figure S5). This
504 difference in behavior with expression levels strongly suggests that the balance
505 between damage and repair rates during transcription differs between germline
506 and soma.

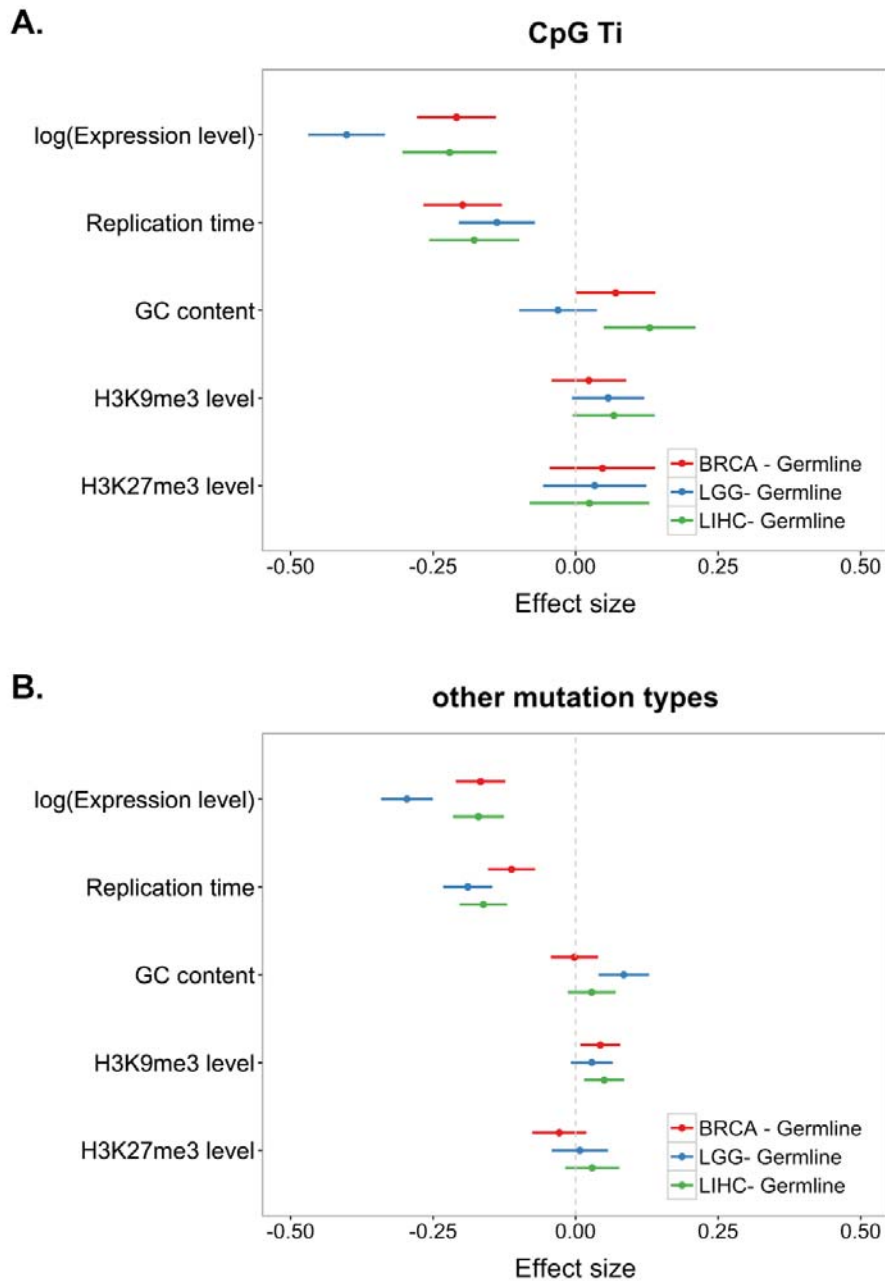
507

Figures



508

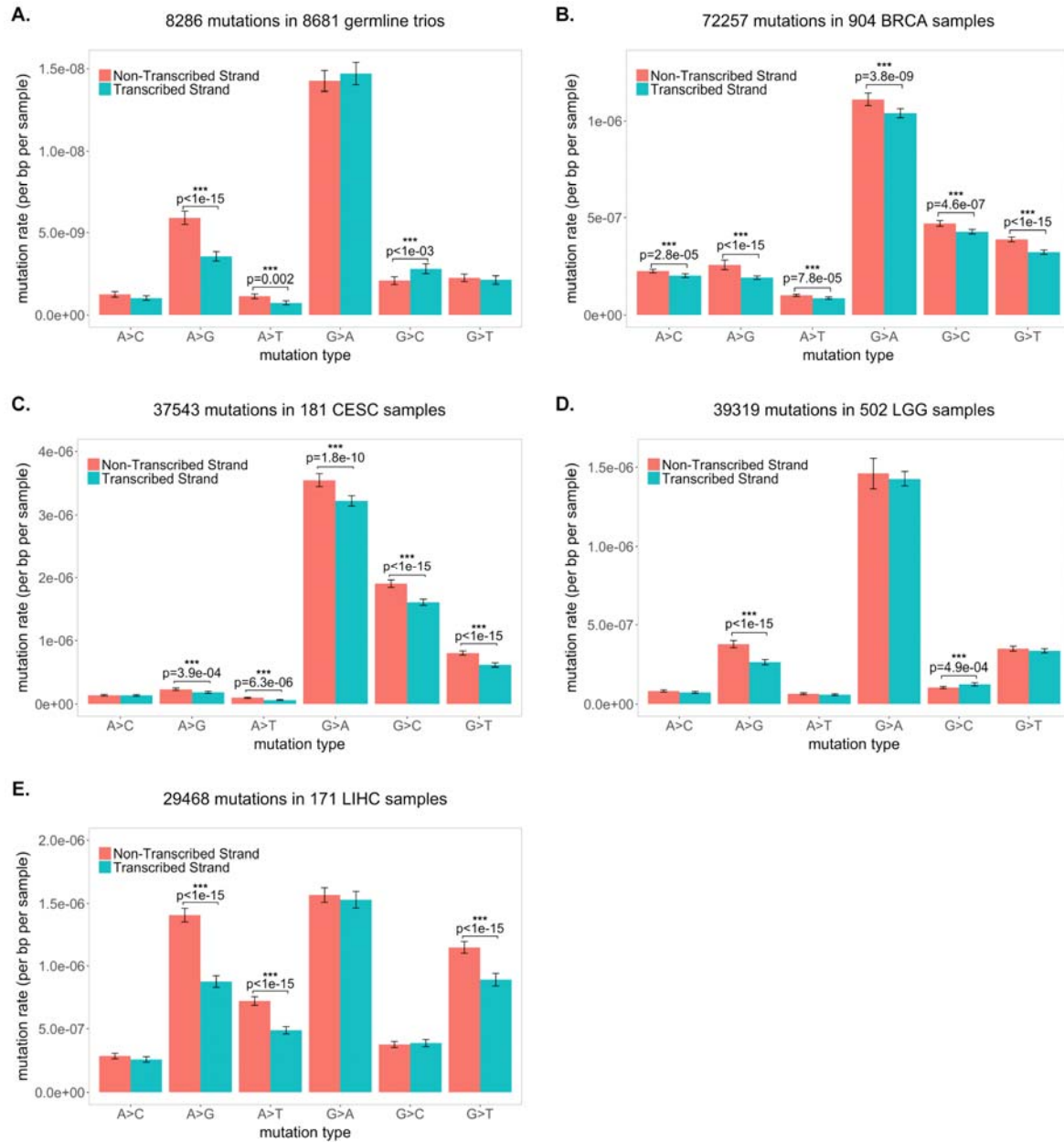
509 **Figure 1.** Coefficients of multivariable binomial regression model fit to germline and somatic
510 mutation data. In panel A, are results for CpG Ti and in panel B, for other mutation types. Red,
511 blue and green, purple and orange bars represent the 95% CI for the estimate of the regression
512 coefficient in germline data set using ovary expression and testis expression, BRCA (breast
513 invasive carcinoma), LGG (brain lower grade glioma) and LIHC (liver hepatocellular carcinoma)
514 data sets respectively. For all replication timing data, high value means early.



515

516 **Figure 2.** Coefficients of combined model comparing each somatic data set to germline data set
517 using testis expression. In panel A, results for CpG Ti and in panel B, for other mutation types.

518 Red, blue and green bars represent the 95% CI of the deviation of the estimated coefficient from
519 the germline estimate; they are shown for BRCA (breast invasive carcinoma), LGG (brain lower
520 grade glioma) and LIHC (liver hepatocellular carcinoma) data sets respectively. For all replication
521 timing data, high value means early.



522

523

Figure 3. Strand asymmetry for six mutation types. In panel A are results for the germline; in

524

panel B, for BRCA (breast invasive carcinoma); in panel C, for CESC (cervical squamous cell

525

carcinoma and endocervical adenocarcinoma); in panel D, for LGG (brain lower grade glioma);

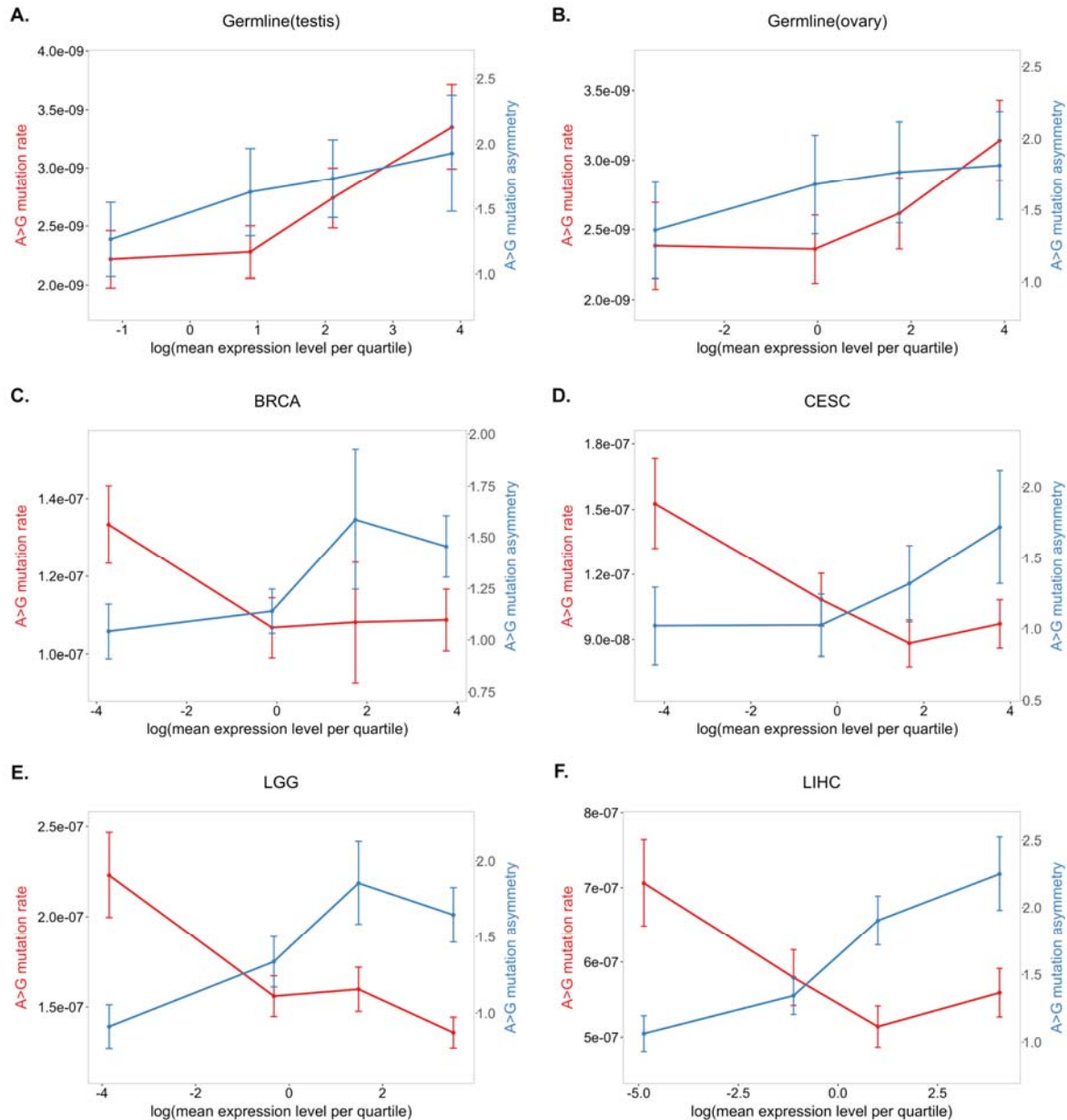
526

and in panel E, for LIHC (liver hepatocellular carcinoma). The error bars of the mutation rate

527

denote 95% confidence intervals estimated by bootstrapping (see Materials and Methods).

528



529

530 **Figure 4.** The degree of A>G strand asymmetry and the A>G mutation rate as a function of gene

531 expression level quartiles. Shown are in panels A and B are results for the germline using testis

532 expression levels and ovary expression levels, respectively; in panel C, for BRCA (breast

533 invasive carcinoma); in panel D, for CESC (cervical squamous cell carcinoma and endocervical

534 adenocarcinoma); in panel E, for LGG (brain lower grade glioma); and in panel F, for LIHC (liver

535 hepatocellular carcinoma). The error bars for both the strand asymmetry and the mutation rate

536 per quartile were estimated by bootstrapping (see Materials and Methods).

537

Discussion

538

539 We compared the determinants of mutation in the soma and the germline, using
540 the same unit of analysis (a coding region) and the same statistical model, and
541 applied it to similar exome data for germline de novo mutations and four types of
542 tumors, in which mutations largely predate tumorigenesis. We recapitulated
543 previous findings of the effects of GC content and of a histone mark indicative of
544 repression on germline and somatic mutations, as well as those of expression
545 levels and replicating time on somatic mutations (Schuster-Böckler and Lehner
546 2012; Lawrence et al. 2013). Strikingly, we also found clear differences in the
547 determinants of mutation rates between germline and soma, consistent with
548 earlier hints based on divergence data (Hodgkinson and Eyre-Walker 2011).
549 Notably, our results confirmed that somatic mutation rates decrease with
550 expression levels and reveal that, in sharp contrast, de novo germline mutation
551 rates increase with expression. This contrast suggests that transcription is
552 mutagenic in germline but not in soma, and that the DNA damage or repair
553 processes differ between them.

554

555 One limitation of our comparison—and of previous studies of germline and
556 somatic mutation—is the need to rely on proxies for determinants of interest,
557 such as replication timing data from cancer cell lines instead of normal cells. A
558 second limitation is that we considered only two types of mutations (CpG Ti and
559 other). Other work indicates that while these two types capture most of the

560 variation in mutation rates, the larger context (adjacent base pairs, but also
561 7mers) also impacts mutation rates (Hwang and Green 2004; Hodgkinson and
562 Eyre-Walker 2011; Aggarwala and Voight 2016). These different mutation
563 subtypes are likely affected somewhat differently by the determinants considered
564 here (Carlson et al. 2017). Despite these limitations, our work provides a
565 framework to contrast possible determinants of mutation rates in soma and
566 germline while controlling for some confounding effects, and results will only
567 improve as data sets increase and the measurements of salient genomic and
568 cellular features become more accurate. What is already clear is that the
569 divergent effect of expression on mutation rates in germline and soma is not
570 attributable to well-known covariates (included in our model). Moreover, the
571 differences that cannot readily be explained by the noise introduced by imperfect
572 proxies or limited data.

573

574 Notably, our results indicate that the tradeoff between damage and repair
575 associated with transcription must differ between germline and soma.
576 Transcription plausibly increases the rate of damage by opening up the DNA
577 helix, rendering the single strands more susceptible to mutagens (Polak and
578 Arndt 2008; Jinks-Robertson and Bhagwat 2014). One possibility is that, in the
579 germline, the rate of transcription-associated mutagenesis (TAM) swamps TCR,
580 leading to higher mutation rates with increased transcription, whereas in the
581 soma, TCR is relatively more efficient and the balance of TAM and TCR leads to
582 decreased mutagenesis with increased expression. Another possibility, which is

583 not mutually exclusive, is the presence of additional repair mechanisms in
584 somatic tissues. In support of this possibility, global genome repair (GGR) is
585 attenuated in differentiated cells, yet mutations on the NTS appear to
586 nonetheless be repaired efficiently (Nospikel and Hanawalt 2000; Marteijn et al.
587 2014). This evidence led to the hypothesis of transcription-domain-associated
588 repair (DAR), which might repair damage on both strands in addition to TCR
589 (reviewed in Nospikel 2007). From an evolutionary standpoint, the increased
590 efficiency of TCR relative to TAM in soma versus germline may be explained by
591 selection pressure on the repair of somatic tissues to prevent aging and cancer
592 (Lynch 2010).

593

594 Mounting evidence suggests that per cell division mutation rates differ across
595 tissues (Greenman et al. 2007; Lynch 2010; Alexandrov et al. 2013) and in
596 particular that they may be higher in early embryonic development than at other
597 stages of development (Ségurel, Wyman, and Przeworski 2014; Rahbari et al.
598 2016; Harland et al. 2016; Lindsay et al. 2016). This study further suggests that
599 at least part of the explanation may lie in the balance between damage and
600 repair, with TCR operating at different efficiencies relative to TAM or jointly with
601 other repair pathways, thereby maintaining low mutation rates in soma. As
602 mutation data from more tissues become available, it will be both feasible and
603 enlightening to examine tissue-specific differences in repair.

604

605

Acknowledgments

606 We thank Ziyue Gao and Priya Moorjani for comments on the manuscripts and
607 helpful discussions.

608

References

- 609 Aggarwala, Varun, and Benjamin F. Voight. 2016. "An Expanded Sequence
610 Context Model Broadly Explains Variability in Polymorphism Levels across
611 the Human Genome." *Nature Genetics* 48 (4): 349–55.
612 doi:10.1038/ng.3511.
- 613 Alexandrov, Ludmil B., Philip H. Jones, David C. Wedge, Julian E. Sale, Peter J.
614 Campbell, Serena Nik-Zainal, and Michael R. Stratton. 2015. "Clock-like
615 Mutational Processes in Human Somatic Cells." *Nature Genetics* 47 (12):
616 1402–7. doi:10.1038/ng.3441.
- 617 Alexandrov, Ludmil, Nik-Zainal Serena, David Wedge, Samuel Aparicio, Sam
618 Behjati, Andrew Biankin, Graham Bignell, et al. 2013. "Signatures of
619 Mutational Processes in Human Cancer." *Nature* 500 (7463): 415–21.
620 doi:10.1038/nature12477.
- 621 Behjati, Sam, Meritxell Huch, Ruben van Boxtel, Wouter Karthaus, David C.
622 Wedge, Asif U. Tamuri, Iñigo Martincorena, et al. 2014. "Genome
623 Sequencing of Normal Cells Reveals Developmental Lineages and
624 Mutational Processes." *Nature* 513 (7518): 422–25.
625 doi:10.1038/nature13448.
- 626 Besenbacher, Søren, Patrick Sulem, Agnar Helgason, Hannes Helgason, Helgi
627 Kristjansson, Aslaug Jonasdottir, Adalbjorg Jonasdottir, et al. 2016. "Multi-
628 Nucleotide de Novo Mutations in Humans." *PLOS Genetics* 12 (11):
629 e1006315. doi:10.1371/journal.pgen.1006315.

- 630 Blokzijl, Francis, Joep de Ligt, Myrthe Jager, Valentina Sasselli, Sophie Roerink,
631 Nobuo Sasaki, Meritxell Huch, et al. 2016. "Tissue-Specific Mutation
632 Accumulation in Human Adult Stem Cells during Life." *Nature* 538 (7624):
633 260–64. doi:10.1038/nature19768.
- 634 Bloom, L. B., M. R. Otto, R. Eritja, L. J. Reha-Krantz, M. F. Goodman, and J. M.
635 Beechem. 1994. "Pre-Steady-State Kinetic Analysis of Sequence-
636 Dependent Nucleotide Excision by the 3'-exonuclease Activity of
637 Bacteriophage T4 DNA Polymerase." *Biochemistry* 33 (24): 7576–86.
- 638 Brennan, Cameron W, Roel Verhaak, McKenna Aaron, Benito Campos, Houtan
639 Noushmehr, Sofie R Salama, Siyuan Zheng, et al. 2013. "The Somatic
640 Genomic Landscape of Glioblastoma." 155 (2): 462–77.
641 doi:10.1016/j.cell.2013.09.034.
- 642 Campbell, Catarina D, and Evan E Eichler. 2013. "Properties and Rates of
643 Germline Mutations in Humans" 29 (10): 575–84.
644 doi:10.1016/j.tig.2013.04.005.
- 645 Carlson, Jedidiah, Laura J. Scott, Adam E. Locke, Matthew Flickinger, Shawn
646 Levy, The BRIDGES Consortium, Richard M. Myers, et al. 2017.
647 "Extremely Rare Variants Reveal Patterns of Germline Mutation Rate
648 Heterogeneity in Humans." *bioRxiv*, February, 108290.
649 doi:10.1101/108290.
- 650 De Rubeis, Silvia, Xin He, Arthur P. Goldberg, Christopher S. Poultney, Kaitlin
651 Samocha, A. Ercument Cicek, Yan Kou, et al. 2014. "Synaptic,

- 652 Transcriptional and Chromatin Genes Disrupted in Autism.” *Nature* 515
653 (7526): 209–15. doi:10.1038/nature13772.
- 654 Duret, Laurent, and Nicolas Galtier. 2009. “Biased Gene Conversion and the
655 Evolution of Mammalian Genomic Landscapes.” *Annual Review of*
656 *Genomics and Human Genetics* 10 (1): 285–311. doi:10.1146/annurev-
657 genom-082908-150001.
- 658 Elango, Navin, Seong-Ho Kim, NISC Comparative Sequencing Program, Eric
659 Vigoda, and Soojin V. Yi. 2008. “Mutations of Different Molecular Origins
660 Exhibit Contrasting Patterns of Regional Substitution Rate Variation.”
661 *PLOS Computational Biology* 4 (2): e1000015.
662 doi:10.1371/journal.pcbi.1000015.
- 663 Epi4K Consortium, and Epilepsy Phenome/Genome Project. 2013. “De Novo
664 Mutations in Epileptic Encephalopathies.” *Nature* 501 (7466): 217–21.
665 doi:10.1038/nature12439.
- 666 Francioli, Laurent C., Paz P. Polak, Amnon Koren, Androniki Menelaou, Sung
667 Chun, Ivo Renkens, Genome of the Netherlands Consortium, et al. 2015.
668 “Genome-Wide Patterns and Properties of de Novo Mutations in Humans.”
669 *Nature Genetics* 47 (7): 822–26. doi:10.1038/ng.3292.
- 670 Fryxell, Karl J., and Won-Jong Moon. 2005. “CpG Mutation Rates in the Human
671 Genome Are Highly Dependent on Local GC Content.” *Molecular Biology*
672 *and Evolution* 22 (3): 650–58. doi:10.1093/molbev/msi043.

- 673 Gao, Ziyue, Minyoung J. Wyman, Guy Sella, and Molly Przeworski. 2016.
674 “Interpreting the Dependence of Mutation Rates on Age and Time.” *PLOS*
675 *Biology* 14 (1): e1002355. doi:10.1371/journal.pbio.1002355.
- 676 Goldmann, Jakob M, Wendy SW Wong, Michele Pinelli, Terry Farrah, Dale
677 Bodian, Anna B Stittrich, Gustavo Glusman, et al. 2016. “Parent-of-Origin-
678 Specific Signatures of de Novo Mutations” 48 (8): 935–39.
679 doi:10.1038/ng.3597.
- 680 Green, Phil, Brent Ewing, Webb Miller, Pamela J. Thomas, NISC Comparative
681 Sequencing Program, and Eric D. Green. 2003. “Transcription-Associated
682 Mutational Asymmetry in Mammalian Evolution.” *Nature Genetics* 33 (4):
683 514–17. doi:10.1038/ng1103.
- 684 Greenman, Christopher, Philip Stephens, Raffaella Smith, Gillian L Dalglish,
685 Christopher Hunter, Graham Bignell, Helen Davies, et al. 2007. “Patterns
686 of Somatic Mutation in Human Cancer Genomes.” *Cah Rev The* 446
687 (7132): 153–58. doi:10.1038/nature05610.
- 688 Hamdan, Fadi F., Myriam Srour, Jose-Mario Capo-Chichi, Hussein Daoud,
689 Christina Nassif, Lysanne Patry, Christine Massicotte, et al. 2014. “De
690 Novo Mutations in Moderate or Severe Intellectual Disability.” *PLOS*
691 *Genetics* 10 (10): e1004772. doi:10.1371/journal.pgen.1004772.
- 692 Hanawalt, Philip C, and Graciela Spivak. 2008. “Transcription-Coupled DNA
693 Repair: Two Decades of Progress and Surprises” 9 (12): 958–70.
694 doi:10.1038/nrm2549.

- 695 Harland, Chad, Carole Charlier, Latifa Karim, Nadine Cambisano, Manon
696 Deckers, Erik Mullaart, Wouter Coppieters, and Michel Georges. 2016.
697 “Frequency of Mosaicism Points towards Mutation-Prone Early Cleavage
698 Cell Divisions.” *bioRxiv*, October, 79863. doi:10.1101/079863.
- 699 Hodgkinson, Alan, Ying Chen, and Adam Eyre-Walker. 2012. “The Large-scale
700 Distribution of Somatic Mutations in Cancer Genomes” 33 (1): 136–43.
701 doi:10.1002/humu.21616.
- 702 Hodgkinson, Alan, and Adam Eyre-Walker. 2011. “Variation in the Mutation Rate
703 across Mammalian Genomes.” *Nat Rev Genetics* 12 (11): 756–66.
704 doi:10.1038/nrg3098.
- 705 Homsy, Jason, Samir Zaidi, Yufeng Shen, James S. Ware, Kaitlin E. Samocha,
706 Konrad J. Karczewski, Steven R. DePalma, et al. 2015. “De Novo
707 Mutations in Congenital Heart Disease with Neurodevelopmental and
708 Other Congenital Anomalies.” *Science* 350 (6265): 1262–66.
709 doi:10.1126/science.aac9396.
- 710 Hwang, Dick G., and Phil Green. 2004. “Bayesian Markov Chain Monte Carlo
711 Sequence Analysis Reveals Varying Neutral Substitution Patterns in
712 Mammalian Evolution.” *Proceedings of the National Academy of Sciences
713 of the United States of America* 101 (39): 13994–1.
714 doi:10.1073/pnas.0404142101.
- 715 Iossifov, Ivan, Brian J. O’Roak, Stephan J. Sanders, Michael Ronemus, Niklas
716 Krumm, Dan Levy, Holly A. Stessman, et al. 2014. “The Contribution of de

- 717 Novo Coding Mutations to Autism Spectrum Disorder.” *Nature* 515 (7526):
718 216–21. doi:10.1038/nature13908.
- 719 Jinks-Robertson, Sue, and Ashok S. Bhagwat. 2014. “Transcription-Associated
720 Mutagenesis.” *Annual Review of Genetics* 48 (1): 341–59.
721 doi:10.1146/annurev-genet-120213-092015.
- 722 Kong, Augustine, Michael L. Frigge, Gisli Masson, Soren Besenbacher, Patrick
723 Sulem, Gisli Magnusson, Sigurjon A. Gudjonsson, et al. 2012. “Rate of de
724 Novo Mutations and the Importance of Father’s Age to Disease Risk.”
725 *Nature* 488 (7412): 471–75. doi:10.1038/nature11396.
- 726 Koren, Amnon, Paz Polak, James Nemesh, Jacob J. Michaelson, Jonathan
727 Sebat, Shamil R. Sunyaev, and Steven A. McCarroll. 2012. “Differential
728 Relationship of DNA Replication Timing to Different Forms of Human
729 Mutation and Variation.” *The American Journal of Human Genetics* 91 (6):
730 1033–40. doi:10.1016/j.ajhg.2012.10.018.
- 731 Larsson, Thomas P., Christian G. Murray, Tobias Hill, Robert Fredriksson, and
732 Helgi B. Schiöth. 2005. “Comparison of the Current RefSeq, Ensembl and
733 EST Databases for Counting Genes and Gene Discovery.” *FEBS Letters*
734 579 (3): 690–98. doi:10.1016/j.febslet.2004.12.046.
- 735 Lawrence, Michael S, Petar Stojanov, Paz Polak, Gregory V Kryukov, Kristian
736 Cibulskis, Andrey Sivachenko, Scott L Carter, et al. 2013. “Mutational
737 Heterogeneity in Cancer and the Search for New Cancer-Associated
738 Genes.” *Nature* 499 (7457): 214–18. doi:10.1038/nature12213.

- 739 Lee, William, Zhaoshi Jiang, Jinfeng Liu, Peter M. Haverly, Yinghui Guan,
740 Jeremy Stinson, Peng Yue, et al. 2010. "The Mutation Spectrum Revealed
741 by Paired Genome Sequences from a Lung Cancer Patient." *Nature* 465
742 (7297): 473–77. doi:10.1038/nature09004.
- 743 Ligt, Joep de, Marjolein H. Willemsen, Bregje W.M. van Bon, Tjitske Kleefstra,
744 Helger G. Yntema, Thessa Kroes, Anneke T. Vulto-van Silfhout, et al.
745 2012. "Diagnostic Exome Sequencing in Persons with Severe Intellectual
746 Disability." *New England Journal of Medicine* 367 (20): 1921–29.
747 doi:10.1056/NEJMoa1206524.
- 748 Lindsay, Sarah J., Raheleh Rahbari, Joanna Kaplanis, Thomas Keane, and
749 Matthew Hurles. 2016. "Striking Differences in Patterns of Germline
750 Mutation between Mice and Humans." *bioRxiv*, October, 82297.
751 doi:10.1101/082297.
- 752 Lodato, Michael A, Mollie B Woodworth, Semin Lee, Gilad D Evrony, Bhaven K
753 Mehta, Amir Karger, Soohyun Lee, et al. 2015. "Somatic Mutation in
754 Single Human Neurons Tracks Developmental and Transcriptional
755 History" 350 (6256): 94–98. doi:10.1126/science.aab1785.
- 756 Lynch, Michael. 2010. "Rate, Molecular Spectrum, and Consequences of Human
757 Mutation." *Proc National Acad Sci* 107 (3): 961–68.
758 doi:10.1073/pnas.0912629107.
- 759 Marteijn, Jurgen A., Hannes Lans, Wim Vermeulen, and Jan H. J. Hoeijmakers.
760 2014. "Understanding Nucleotide Excision Repair and Its Roles in Cancer

- 761 and Ageing.” *Nature Reviews Molecular Cell Biology* 15 (7): 465–81.
762 doi:10.1038/nrm3822.
- 763 Martincorena, Iñigo, Amit Roshan, Moritz Gerstung, Peter Ellis, Peter Loo,
764 McLaren Stuart, David C Wedge, et al. 2015. “High Burden and Pervasive
765 Positive Selection of Somatic Mutations in Normal Human Skin” 348
766 (6237): 880–86. doi:10.1126/science.aaa6806.
- 767 McVicker, Graham, David Gordon, Colleen Davis, and Phil Green. 2009.
768 “Widespread Genomic Signatures of Natural Selection in Hominid
769 Evolution.” *PLOS Genetics* 5 (5): e1000471.
770 doi:10.1371/journal.pgen.1000471.
- 771 McVicker, Graham, and Phil Green. 2010. “Genomic Signatures of Germline
772 Gene Expression.” *Genome Research* 20 (11): 1503–11.
773 doi:10.1101/gr.106666.110.
- 774 Michaelson, Jacob J, Yujian Shi, Madhusudan Gujral, Hancheng Zheng, Dheeraj
775 Malhotra, Xin Jin, Minghan Jian, et al. 2012. “Whole-Genome Sequencing
776 in Autism Identifies Hot Spots for De Novo Germline Mutation” 151 (7):
777 1431–42. doi:10.1016/j.cell.2012.11.019.
- 778 Moorjani, Priya, Ziyue Gao, and Molly Przeworski. 2016. “Human Germline
779 Mutation and the Erratic Evolutionary Clock.” *PLOS Biology* 14 (10):
780 e2000744. doi:10.1371/journal.pbio.2000744.
- 781 Muller, H. J. 1927. “ARTIFICIAL TRANSMUTATION OF THE GENE.” *Science* 66
782 (1699): 84–87. doi:10.1126/science.66.1699.84.

- 783 Nospikel, Thierry. 2007. "DNA Repair in Differentiated Cells: Some New
784 Answers to Old Questions." *Neuroscience, Genome Dynamics and DNA*
785 *Repair in the CNS*, 145 (4): 1213–21.
786 doi:10.1016/j.neuroscience.2006.07.006.
- 787 Nospikel, Thierry. 2009. "DNA Repair in Mammalian Cells." *Cellular and*
788 *Molecular Life Sciences* 66 (6): 994–1009. doi:10.1007/s00018-009-8737-
789 y.
- 790 Nospikel, Thierry, and Philip C. Hanawalt. 2000. "Terminally Differentiated
791 Human Neurons Repair Transcribed Genes but Display Attenuated Global
792 DNA Repair and Modulation of Repair Gene Expression." *Molecular and*
793 *Cellular Biology* 20 (5): 1562–70.
- 794 Park, Chungoo, Wenfeng Qian, and Jianzhi Zhang. 2012. "Genomic Evidence for
795 Elevated Mutation Rates in Highly Expressed Genes." *EMBO Reports* 13
796 (12): 1123–29. doi:10.1038/embor.2012.165.
- 797 Petruska, J., and M. F. Goodman. 1985. "Influence of Neighboring Bases on
798 DNA Polymerase Insertion and Proofreading Fidelity." *Journal of*
799 *Biological Chemistry* 260 (12): 7533–39.
- 800 Pleasance, Erin D., R. Keira Cheetham, Philip J. Stephens, David J. McBride,
801 Sean J. Humphray, Chris D. Greenman, Ignacio Varela, et al. 2010. "A
802 Comprehensive Catalogue of Somatic Mutations from a Human Cancer
803 Genome." *Nature* 463 (7278): 191–96. doi:10.1038/nature08658.
- 804 Pleasance, Erin D., Philip J. Stephens, Sarah O'Meara, David J. McBride, Alison
805 Meynert, David Jones, Meng-Lay Lin, et al. 2010. "A Small-Cell Lung

- 806 Cancer Genome with Complex Signatures of Tobacco Exposure.” *Nature*
807 463 (7278): 184–90. doi:10.1038/nature08629.
- 808 Polak, Paz, and Peter F. Arndt. 2008. “Transcription Induces Strand-Specific
809 Mutations at the 5’ End of Human Genes.” *Genome Research* 18 (8):
810 1216–23. doi:10.1101/gr.076570.108.
- 811 Polak, Paz, Rosa Karlič, Amnon Koren, Robert Thurman, Richard Sandstrom,
812 Michael Lawrence, Alex Reynolds, et al. 2015. “Cell-of-Origin Chromatin
813 Organization Shapes the Mutational Landscape of Cancer.” *Nature* 518
814 (7539): 360–64. doi:10.1038/nature14221.
- 815 Rahbari, Raheleh, Arthur Wuster, Sarah Lindsay, Robert Hardwick, Ludmil
816 Alexandrov, Saeed Turki, Anna Dominiczak, et al. 2016. “Timing, Rates
817 and Spectra of Human Germline Mutation.” *Nat Genet* 48 (2): 126–33.
818 doi:10.1038/ng.3469.
- 819 Rauch, Anita, Dagmar Wieczorek, Elisabeth Graf, Thomas Wieland, Sabine
820 Ende, Thomas Schwarzmayr, Beate Albrecht, et al. 2012. “Range of
821 Genetic Mutations Associated with Severe Non-Syndromic Sporadic
822 Intellectual Disability: An Exome Sequencing Study.” *The Lancet* 380
823 (9854): 1674–82. doi:10.1016/S0140-6736(12)61480-9.
- 824 Rubin, Alan F., and Phil Green. 2009. “Mutation Patterns in Cancer Genomes.”
825 *Proceedings of the National Academy of Sciences* 106 (51): 21766–70.
826 doi:10.1073/pnas.0912499106.
- 827 Samocha, Kaitlin E, Elise B Robinson, Stephan J Sanders, Christine Stevens,
828 Aniko Sabo, Lauren M McGrath, Jack A Kosmicki, et al. 2014. “A

- 829 Framework for the Interpretation of de Novo Mutation in Human Disease.”
830 *Nature Genetics* 46 (9): 944–50. doi:10.1038/ng.3050.
- 831 Schuster-Böckler, Benjamin, and Ben Lehner. 2012. “Chromatin Organization Is
832 a Major Influence on Regional Mutation Rates in Human Cancer Cells”
833 488 (7412): 504–7. doi:10.1038/nature11273.
- 834 Ségurel, Laure, Minyoung J. Wyman, and Molly Przeworski. 2014. “Determinants
835 of Mutation Rate Variation in the Human Germline.” *Annual Review of*
836 *Genomics and Human Genetics* 15: 47–70. doi:10.1146/annurev-genom-
837 031714-125740.
- 838 Shendure, Jay, and Joshua M. Akey. 2015. “The Origins, Determinants, and
839 Consequences of Human Mutations.” *Science* 349 (6255): 1478–83.
840 doi:10.1126/science.aaa9119.
- 841 Stamatoyannopoulos, John A., Ivan Adzhubei, Robert E. Thurman, Gregory V.
842 Kryukov, Sergei M. Mirkin, and Shamil R. Sunyaev. 2009. “Human
843 Mutation Rate Associated with DNA Replication Timing.” *Nature Genetics*
844 41 (4): 393–95. doi:10.1038/ng.363.
- 845 Stratton, Michael R. 2011. “Exploring the Genomes of Cancer Cells: Progress
846 and Promise.” *Science* 331 (6024): 1553–58.
847 doi:10.1126/science.1204040.
- 848 Stratton, Michael R., Peter J. Campbell, and P. Andrew Futreal. 2009. “The
849 Cancer Genome.” *Nature* 458 (7239): 719–24. doi:10.1038/nature07943.

- 850 Supek, Fran, and Ben Lehner. 2015. "Differential DNA Mismatch Repair
851 Underlies Mutation Rate Variation across the Human Genome" 521
852 (7550): 81–84. doi:10.1038/nature14173.
- 853 Takai, Daiya, and Peter A. Jones. 2002. "Comprehensive Analysis of CpG
854 Islands in Human Chromosomes 21 and 22." *Proceedings of the National
855 Academy of Sciences* 99 (6): 3740–45. doi:10.1073/pnas.052410099.
- 856 The Deciphering Developmental Disorders Study. 2015. "Large-Scale Discovery
857 of Novel Genetic Causes of Developmental Disorders." *Nature* 519 (7542):
858 223–28. doi:10.1038/nature14135.
- 859 Webster, Matthew T., Nick G. C. Smith, Martin J. Lercher, and Hans Ellegren.
860 2004. "Gene Expression, Synteny, and Local Similarity in Human
861 Noncoding Mutation Rates." *Molecular Biology and Evolution* 21 (10):
862 1820–30. doi:10.1093/molbev/msh181.
- 863 Zhao, Shanrong, and Baohong Zhang. 2015. "A Comprehensive Evaluation of
864 Ensembl, RefSeq, and UCSC Annotations in the Context of RNA-Seq
865 Read Mapping and Gene Quantification." *BMC Genomics* 16 (1): 97.
866 doi:10.1186/s12864-015-1308-8.